Magneto-optical determination of exciton binding energies in quantum-wire superlattices

H. Weman*
Department of Physics and Measurement Technology, Linköping University, S-581 83 Linköping, Sweden

M. Potemski
High Magnetic Field Laboratory, Max-Planck-Institut für Festkörperforschung and Centre National de la Recherche Scientifique, F 38042 Grenoble, France

M. E. Lazzouni
Department of Physics, University of California San Diego, La Jolla, California 92093

M. S. Miller[†] and J. L. Merz[‡]
Center for Quantized Electronic Structures, University of California, Santa Barbara, California 93106
(Received 3 November 1995)

Polarization-resolved photoluminescence excitation spectra of (Al, Ga)As serpentine superlattice quantum-wire arrays have been measured in magnetic fields up to 20 T. In the Faraday configuration we are able to resolve Landau-level-like magnetoexciton transitions in the low-field limit, and to directly determine the exciton binding energy. A maximum enhancement of excitonic binding by 70% is observed in a 160-Å-wide quantum wire array as compared to a two-dimensional reference, and the true superlattice character is evidenced by a decreased excitonic binding for a short period (54 Å wide) compared to a long period quantum-wire array (160 Å wide).

Linearly polarized luminescence can be a signature of one-dimensional (1D) carrier confinement in semiconductor quantum wires.[1–5] The polarization, though, is not a sufficient property for demonstrating the 1D character of the electronic structure. Additional information is obtained when the photoluminescence (PL) is measured in a magnetic field. For example, the anisotropic diamagnetic shift seen in the magneto-PL of quantum-wire excitons reveals both the length scale and the anisotropic nature of the electronic structure, where in the low-field regime the cyclotron orbit is larger than the confining structure, and in the high-field regime the cyclotron orbit is smaller.[6,7] An important energy in the problem is the binding energy of the confined exciton. The binding energy may be measured in the low-field limit by measuring the magneto-PL shift,[6] though localization will lead to an overestimation of the binding energy. In the high-field limit a binding energy can be measured through an analysis of Landau-level-like magnetoexciton spectra.[2] However, such a measurement reflects excitons confined by the magnetic field and not by the 1D potential. Isolated quantum wires are one member from a class of ''1D'' systems, which also includes coupled wires and periodic arrays of coupled wires. This 1D class is analogous to the 2D class, which includes quantum wells, coupled quantum wells, and superlattices. While an array of quantum wires will share some electronic structure features with isolated quantum wires, the band structure due to periodicity and coupling will give rise to additional novel properties. Specifically of interest here is that the superlattice minibands in a sheet of wires allow Landau-like levels in the low-field regime for a magnetic field perpendicular to the sheet, and the binding energy for excitons confined by the 1D array potential can then be extracted.

In this paper we report the binding energy of excitons in coupled quantum-wire arrays directly determined from magnetoexciton excitation spectra observed in the low-field limit. The coupled quantum-wire arrays are those found in a serpentine superlattice (SSL). Our results here show a strong enhancement of excitonic binding in the SSL quantum wire arrays as compared to a 2D reference, and the true superlattice character is evidenced by a decreased excitonic binding for a short-period (strong-coupling regime) compared to a long-period quantum-wire array (weak-coupling regime), in good agreement with theoretical calculations.

Serpentine superlattices result from a growth technique that uses the atomic step edges of a vicinal surface as templates for 1D growth. The wires are defined by curving boundaries (with a radius of curvature r) between lateral-well and -barrier materials with the 1D states in the wide parts of the wells. The confinement can be characterized by the aspect ratio $f=a/b$, where a is the vertical distance measured at the midpoint between the barriers and b is the lateral distance between the barriers, as shown in the inset of Fig. 1. The SSL structures used in our experiments have been grown on 0.5° and 1.5° misoriented vicinal (100) GaAs substrates, corresponding to a stepped surface with a terrace width of 324 and 108 Å, respectively. The anticipated aspect ratios of the confinement regions are therefore $f=0.52$ and 1.6 for the 0.5° and 1.5° SSL, respectively. The deposition sequence corresponded to $Al_xGa_{1-x}As$ barriers of $x_{barrier}=20\%$, which are 1/2-terrace wide. The SSL's have a thickness of 34 nm with a ramping constant $z_0=125$ nm.[8] A reference (2D) sample of the same average composition though with no lateral composition modulation has also been investigated.

Photoluminescence and photoluminescence excitation (PLE) spectra have been measured at 1.6 K in a 10-MW

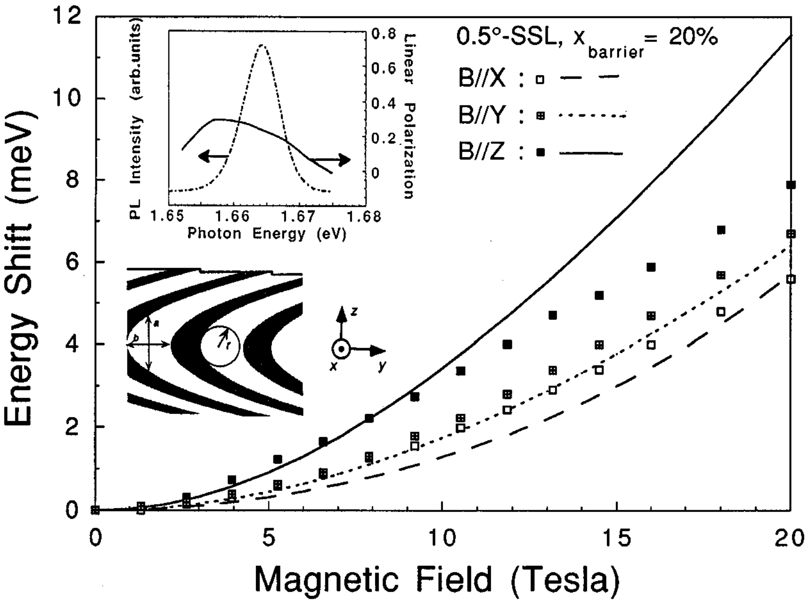

FIG. 1. Experimental data points and calculated energy shift of the 0.5° serpentine superlattice (SSL) emission as a function of the applied magnetic field in the x, y, and z directions. Inset shows the photoluminescence (dash-dotted line) and linear polarization spectrum (solid line) of the luminescence emitted in the z direction. A schematic figure of a SSL structure with a parabolic cross section is also shown, with the parameters a, b, and r defined in the text.

resistive Bitter magnet in fields up to 20 T. For the PL measurements we used the 488-nm line from an Ar^+ laser and for the PLE measurements a Ti:sapphire laser. The emitted light from the sample was dispersed through a 1.5-m Jobin Yvon spectrometer and detected with a GaAs photomultiplier. The magnetic field was applied parallel to the x, y, and z axes, defined as parallel to the wires, in the periodic direction and normal to the array. In the PL (PLE) experiments the direction of the emitted (exciting) light wave vector k was always normal to the vicinal surface (z direction). Applying the magnetic field in the z direction therefore corresponds to the Faraday configuration ($B\|k\|z$) and the x or y direction corresponds to the Voigt configuration ($B\perp k$). In the Faraday configuration the circularly polarized components of the excited as well as the emitted light have been analyzed.

The presence of lateral anisotropy in our structures can already be deduced on the basis of linearly polarized luminescence experiments. The representative PL spectrum (dashed-dotted line) together with the linear polarization of the luminescence in the z direction, $P_z=(I_x-I_y)/(I_x+I_y)$ (solid line) for the 0.5° SSL structure is shown in the inset of Fig. 1. The PL emission is identified as a localized electron (e) heavy-hole (hh) exciton ($e1$hh1) recombining in the SSL layer. The luminescence is polarized parallel to the wires with the maximum of the polarization redshifted from the PL peak. The linear polarization at the PL peak is 25%. The redshift of the polarization maximum shows that there is a distribution of quantum wires of different quality within the PL peak.[8] Introducing a model that allows for intermixing we can determine the height of the lateral potential from the measured polarization at the PL peak.[9] The intermixing has been considered by a rectangular composition profile, where the Al is uniformly removed and uniformly redistributed into the well. The linear polarization has then been calculated for the electron–heavy-hole transition as a function of the difference in the Al composition in the barrier and well.[9] Here we estimate the actual Al composition in the barrier (wire) to be 15% (5%) instead of the intended 20% (0%), giving a lateral potential modulation in the conduction band of 80 meV. The positive linear polarization confirms the 1D-like character of the *heavy hole*, but to determine if the *exciton* also is affected by the lateral potential, we measured the PL shift in three orthogonal magnetic field configurations.

In Fig. 1 the experimental data points of the energy shift of the 0.5° SSL emission as a function of the applied magnetic field are shown. To quantitatively explain the data we calculated the energy shifts for the band-to-band electron–heavy-hole transition, excluding exciton effects.[10] The electron and hole wave functions were computed for free carriers confined in the SSL structure, by solving the 2D Schrödinger equation. In the model we included the intermixing of the barrier and well material, and the best fit to the data was achieved with an Al composition in the barrier (wire) of 16% (4%), as shown by the solid and dashed lines in Fig. 1. The amount of the energy shift is critically dependent on the direction of the applied magnetic field and is in fairly good agreement with the data, except above 10 T in the z direction. These data give a clear indication that the ground-state exciton wave packet is experiencing an anisotropic environment. The fact that the shifts in the x and y directions are different, in contrast to what we observed in the 2D reference, especially apparent in the field range near 20 T, indicate that we have removed the original in-plane isotropy by the lateral potential. However, due to the fact that the excitons observed in PL are strongly localized in potential fluctuations, the magneto-PL shifts cannot be used to accurately deduce the reduced mass or binding energy of the exciton.[11] In fact, reduced diamagnetic shifts observed in quantum wells have been shown to be due to exciton localization.[12] From temperature-dependent luminescence experiments we have estimated the localization potential in the SSL structure to be 10 meV deep.[13] Therefore any determination of the binding energy of the exciton from the magneto-PL shifts will be an overestimation. Even using the PLE shifts to determine the binding energy can be very ambiguous unless the absorption is due to a truly free excitonic state in the wire. Such wires are very difficult (if not impossible) to fabricate with the present technology. In most cases the absorption

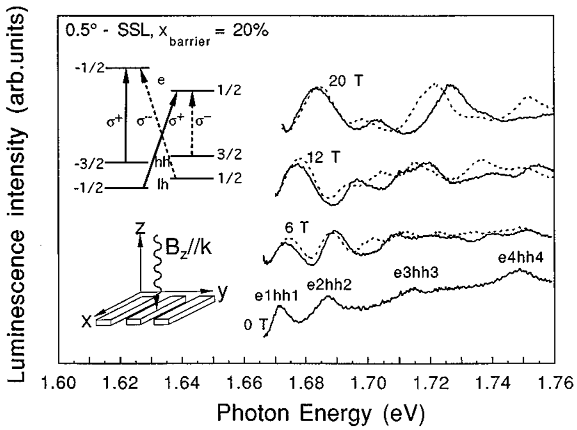

FIG. 2. Left- (σ^-) and right- (σ^+) handed circularly polarized photoluminescence excitation (PLE) spectra for a 0.5° SSL quantum wire in the Faraday configuration. Optical selection rules for allowed PLE transitions between electron heavy-hole and electron light-hole states in a magnetic field ($B\|k\|z$) are shown in the inset.

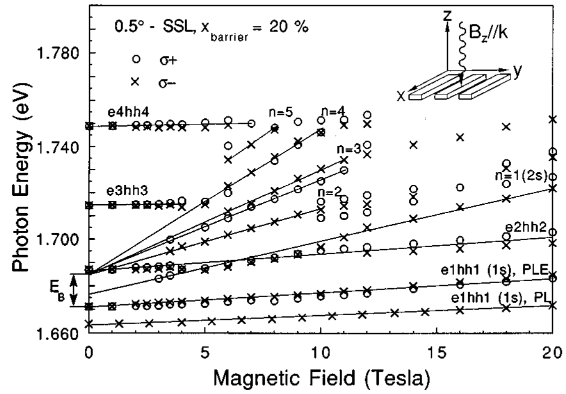

FIG. 3. Fan chart plot of the electron heavy-hole subbands and Landau levels for the 0.5° SSL quantum wire, with arrows indicating the experimentally determined exciton binding energy (here 13.5±0.5 meV). The solid lines connecting the Landau-level-like magnetoexciton transitions ($n=2$, 3, and 4) are linear fits to the data points. The $e1$hh1(1s) PL transition and the four subband transitions are connected by straight lines as a guide to the eye.

will be due to delocalized excitons, which are defined as excitons that are free to move in a region of the wire that is uniform on a length scale larger than the Bohr diameter of the exciton along the wire direction.

In Fig. 2 left- (σ^-) and right- (σ^+) handed circularly polarized PLE spectra of the 0.5° SSL sample are shown with the magnetic field parallel to the z direction (perpendicular to the plane of the quantum-wire superlattice). At zero magnetic fields four peaks can be resolved that are due to the ground-state heavy-hole exciton [$e1$hh1(1s)] (Stokes shifted by 7.5 meV) and excited heavy-hole excitons from higher subbands ($e2$hh2, $e3$hh3, $e4$hh4).[14] By increasing the magnetic field we see several new (spin-split) Landau-level-like magnetoexciton transitions, [$e1$hh1 ($n=1$, 2, 3, 4, and 5)], from fields as low as 3 T. The cyclotron orbit diameter is given by $d=2(h/eB)^{1/2}(2n+1)^{1/2}$, where $n=0,1,2,\ldots$ is the Landau-level quantum number. This means that in the low-field regime where the higher Landau-level-like magnetoexcitons start to appear (3–6 T for $n=2$, 3, 4, and 5) the orbits are actually tunneling through a few lateral barriers. This situation is analogous to the case of a superlattice under an in-plane magnetic field and distinctly different from isolated quantum wires where Landau levels have been found to be quenched when the cyclotron diameter is wider than the wire width.[15]

In Fig. 3 a fan chart is plotted of all the observed transitions in PLE for the 0.5° SSL sample. The $e1$hh1 PL transition and the four subband transitions observed in PLE are connected by straight lines as a guide to the eye. When analyzed in detail they show a quadratic field dependence at low fields as expected for quantum wires in the low-field limit. For the SSL quantum wire we can determine the band edge by a linear extrapolation of the higher ($n=2$, 3, and 4) Landau-level-like transitions to zero field. One can therefore directly determine the binding energy of the delocalized ground-state exciton by subtracting the zero-field [$e1$hh1 (1s)] peak position from the Landau-level band edge. It should be noted that this determination of the band edge by fitting the higher Landau levels is done in the low-field limit where the electrostatic confinement is dominating over the magnetic-field-induced confinement. The excitonic binding energy has previously been determined in a similar way for quantum wells as well as for superlattices.[16,17] By fitting Landau level $n=2$, 3, and 4 in Fig. 3, we determine the exciton binding energy to be 13.5±0.5 meV for the 0.5° SSL sample. The uncertainty of ±0.5 meV comes from the spread of the extrapolated zero-field band-edge energy points after the linear fitting procedure of the higher Landau levels. We have performed similar measurements for the 1.5° SSL sample and for the 2D reference alloy sample. We find the exciton binding energy to be 11.5±0.5 meV in the 1.5° SSL sample and 8.0±0.5 meV in the 2D reference sample.

By using a fractional dimensional approach the $e1$hh1 exciton binding energy, in units of the Rydberg energy, E_0 (4 meV for bulk GaAs),[18] has recently been calculated for GaAs/$Al_{0.15}Ga_{0.85}As$ cylindrical quantum wires as a function of the wire radius in units of the Bohr radius, a_0 (14 nm for bulk GaAs),[18] by Christol, Lefebvre, and Mathieu,[19] shown as the solid line in Fig. 4. Our experimental values for the two SSL samples, using a 3D $Al_{0.05}Ga_{0.95}As$ Rydberg energy of 4.85 meV,[18] are shown by the crosses in Fig. 4. Here we have assumed that the exciton binding energy is related to the cross-sectional area rather than to its geometrical shape, and estimated the wire radius that gives the same cross-sectional area as we have in the SSL wires. This assumption is justified since it has been shown that the exciton binding energy in a quantum wire is determined by the cross-sectional area on which the wave function is concentrated, rather than the shape of the wire.[19,20] The decreased binding energy for the narrowest wire is due to the strong lateral penetration of the exciton wave function into the barrier region and is in good agreement with the calculations by Christol, Lefebvre, and Mathieu.[19]

For comparison we have also included other published values on the exciton binding energy in *isolated* GaAs/$Al_xGa_{1-x}As$ quantum wires in Fig. 4 (with the actual cross section scaled to cylindrical geometry). Kohl *et al.* determined the excitonic binding energy for 700-Å-wide etched GaAs quantum wires, and Nagamune *et al.* and Rinaldi *et al.*

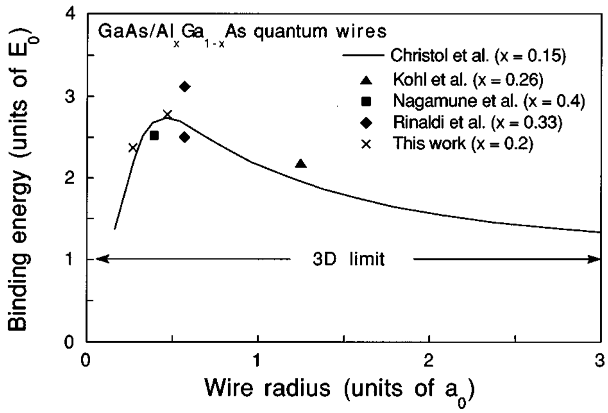

FIG. 4. Calculated binding energy of the $e1$hh1 exciton for cylindrical GaAs/$Al_{0.15}Ga_{0.85}As$ quantum wires by Christol, Lefebvre, and Mathieu (Ref. 19). The experimental data points for the 0.5° and 1.5° SSL sample determined in this work are shown together with the data from Kohl *et al.* (Ref. 2), Nagamune *et al.* (Ref. 6), and Rinaldi *et al.* (Ref. 21). The energy and radius are given in units of the Rydberg energy (E_0) and the Bohr radius (a_0), respectively.

for 200-Å-wide GaAs V-groove wires.[2,6,21] The binding energy determined by Kohl *et al.* was determined in a similar way as for the SSL's, however, in the former case the Landau-level transitions were observed in the high-field limit and therefore do not correctly correspond to the binding energy of the wire. In the study by Nagamune *et al.* an excitonic binding energy of 10.1 meV was determined from the magnetoluminescence shift.[6] Rinaldi *et al.* estimated the binding energy to be 10 meV from two-photon absorption and 12.5 meV by fitting the magnetoluminescence shift.[21] All values are in surprisingly good agreement with the calculations by Christol, Lefebvre, and Mathieu, considering the differences in the x values of the $Al_xGa_{1-x}As$ barrier of the quantum wires and that the comparison is made by approximation of the cross-sectional areas.

We have also measured the PLE spectra with the magnetic field applied along the wire direction ($B\|x$) and in the direction of the superlattice period ($B\|y$). We do not, however, observe any higher excited Landau-level-like magnetoexciton transitions in this geometry, due to the fact that the cyclotron diameter for these transitions is much larger than the vertical width. Instead here the higher subbands approach those of the harmonic oscillator, $[E=h\omega_c(n+1/2)$, where $\omega_c=eB/\mu]$, at high magnetic fields.

In conclusion we have reported on polarization resolved magneto-PLE studies of (Al,Ga)As serpentine superlattice quantum wires. The excitonic binding energies have been directly determined from the analysis of Landau-level-like excited magnetoexciton transitions observed in the low-field limit. A strong enhancement of excitonic binding is observed compared to 2D, with a reduction in the exciton binding energy for very narrow quantum wire arrays. Experiments performed for different orientations of the magnetic field show that the carrier confinement is quantum-well-like in the direction parallel to the growth and superlatticelike in the lateral direction.

We want to thank P. Christol, B. Monemar, L. J. Sham, and P. Wyder for fruitful discussions and interest in this work.

---

*Electronic address: hwn@ifm.liu.se
†Present address: Dept. of Solid State Physics, Lund University, S-221 00 Lund, Sweden.
‡Present address: Dept. of Electrical Engineering, University of Notre Dame, Notre Dame, IN 46556.

1 E. Kapon, D. M. Hwang, and R. Bhat, Phys. Rev. Lett. **63**, 430 (1989).
2 M. Kohl, D. Heitman, P. Grambow, and K. Ploog, Phys. Rev. Lett. **63**, 2124 (1989).
3 D. Gershoni *et al.*, Phys. Rev. Lett. **65**, 1631 (1990).
4 M. Notomi *et al.*, Appl. Phys. Lett. **58**, 720 (1991).
5 M. S. Miller *et al.*, Phys. Rev. Lett. **68**, 3464 (1992).
6 Y. Nagamune *et al.*, Phys. Rev. Lett. **69**, 2963 (1992).
7 H. Weman *et al.*, Superlatt. Microstruct. **13**, 5 (1993).
8 H. Weman *et al.*, Phys. Rev. B **48**, 8047 (1993).
9 C. Pryor, Phys. Rev. B **44**, 12 912 (1991).
10 The PL shift in a magnetic field can be well explained even without including excitonic effects since the change of the exciton binding energy is relatively small compared to the energy shift due to the magnetic field, as shown by T. Tanaka, Y. Arakawa, and G. W. E. Bauer, Phys. Rev. B **50**, 7719 (1994).
11 Localization also explains why the deviation between the calculated and measured PL shift is especially apparent in the z direction at high fields, since here the field shrinking magnetoexciton is "probing" the lateral potential, which we have previously shown to be much less uniform than the vertical potential (see Ref. 7). This model can be understood if the characteristic size of the potential fluctuations is smaller than the size of the magnetoexciton at low fields and comparable to or less than the potential fluctuations at high fields.
12 K. J. Nash, M. S. Skolnick, P. A. Claxton, and J. S. Roberts, Phys. Rev. B **39**, 10 943 (1989).
13 H. Weman *et al.*, Superlatt. Microstruct. **17**, 61 (1995).
14 The ground-state light-hole exciton ($e1$lh1) is partly overlapping and hidden on the high-energy side of the ground-state heavy-hole exciton peak ($e1$hh1). It gives rise to the broadening and apparent absence of excitonic spin splitting of the $e1$hh1 peak at higher fields, according to the energy diagram of the spin splittings of the $e1$hh1 and $e1$lh1 transitions (shown in the inset to Fig. 2).
15 J. Hammersberg, H. Weman, M. Notomi, and T. Tamamura, Superlattices Microstruct. **16**, 143 (1994).
16 D. C. Rogers *et al.*, Phys. Rev. B **34**, 4002 (1986).
17 G. Belle, J. C. Maan, and G. Weimann, Solid State Commun. **56**, 65 (1985).
18 L. Pavesi, *Properties of Gallium Arsenide* [Institution of Electrical Engineers (INSPEC), New York, 1988], p. 530.
19 P. Christol, P. Lefebvre, and H. Mathieu, J. Appl. Phys. **74**, 5626 (1993).
20 M. H. Degani and O. Hipolito, Phys. Rev. B **35**, 9345 (1987).
21 R. Rinaldi *et al.*, Phys. Rev. Lett. **73**, 2899 (1994).